Chromatographic Dynamic Chemisorption

CHROMATOGRAPHIC DYNAMIC CHEMISORPTION

A Thesis Presented

by

Shreya Thakkar

Submitted to the Graduate School of the
University of Massachusetts Amherst in partial fulfillment
of the requirements of the degree of

MASTER OF SCIENCE IN CHEMICAL ENGINEERING

May 2022

Department of Chemical Engineering

CHROMATOGRAPHIC DYNAMIC CHEMISORPTION

A Thesis Presented

by

Shreya Thakkar

Approved as to style and content by:

_____

Omar Abdelrahman, Chair

_____

Friederike Jentoft, Member

_____

Ashwin Ramasubramaniam, Member

_____

Jessica Schiffman, Department Head

Department of Chemical Engineering

ACKNOWLEDGEMENTS

First, I would like to sincerely thank my advisor, Professor Omar Abdelrahman for his guidance at every step. His enthusiasm and immense knowledge in the field were extremely helpful for my research work. His suggestions and thoughts about the experiments and analysis were instrumental in successful completion of this thesis. His experience with analytical instruments was a significant help in troubleshooting.

I would also like to thank my committee members, Professor Friederike Jentoft and Professor Ashwin Ramasubramaniam for their guidance and insightful suggestions.

I am also grateful to all the past and present members of the Abdelrahman lab for their encouragement, support, and suggestions throughout the duration of my research.

Finally, I would also like to extend my gratitude to my parents and close friends for their continued support throughout the duration of my degree.

ABSTRACT

CHROMATOGRAPHIC DYNAMIC CHEMISORPTION

MAY 2022

SHREYA THAKKAR

B.CHEM. ENG. INSTITUTE OF CHEMICAL TECHNOLOGY

M.S. ChE UNIVERSITY OF MASSACHUSETTS, AMHERST

Directed by: Professor Omar Abdelrahman

Reaction rates of catalytic cycles over supported metal catalysts are normalized by the exposed metal atoms on the catalyst surface, reported as site time yields which provide a rigorous standard to compare distinct metal surfaces. Defined as the fraction of exposed metal surface atoms to the total number of metal atoms, it is important to measure the dispersion of supported metal catalysts to report standardized rates for kinetic investigations. Multiple characterization techniques such as electron microscopy, spectroscopy and chemisorption are exploited for catalyst dispersion measurements. While effective, electron microscopy and spectroscopy are not readily accessible due to cost and maintenance requirements. Commercial instruments therefore typically rely on chemisorption measurements, but can be cost prohibitive nonetheless, hindering the ability of catalysis research to report rigorous measures of activity. Thus, a dispersion measurement technique based on gas chromatograph (GC) ubiquitous in catalysis research is proposed, based on the principle of dynamic carbon monoxide (CO) chemisorption, where number of exposed metal surface atoms are estimated based on the amount of adsorbed CO.

In this technique, the supported metal catalyst is packed into a liner, and inserted in the temperature-controlled inlet of the GC. The catalyst is pre-treated, purged with inert gas, and pulses of known amount of CO are passed through it via an automated sequence. The CO chemically adsorbs on the supported metal catalyst and the unadsorbed CO is detected by the flame ionization detector/methanizer on the GC. The amount of CO adsorbed is estimated by the difference between the amount of CO pulsed and detected, translated to estimate the number of exposed metal surface atoms using a stoichiometry factor. Dispersion measurements for several group VIII metal catalysts were conducted using this technique to demonstrate its applicability across a range of weight loadings and support identities. An agreement between catalyst dispersion measured using this technique and commercially available instruments indicated the reliability of this technique. The amount of dispersed metal as low as 0.02 mg could be estimated by this technique.

TABLE OF CONTENTS

LIST OF TABLES

LIST OF FIGURES

CHAPTER 1

INTRODUCTION

1.1 Supported metal catalysts and their dispersion

Metal catalysts have a wide variety of applications such as petroleum refining,[1, 2] synthesis of pharmaceutical products,[3] sustainable energy production via fuel cells,[4] and the automotive industry.[5, 6] Platinum group metals are commonly used metal catalysts and contribute the highest share in the global precious catalyst market.[7] To develop efficient catalysts, the metals are generally incorporated on a support. There are several advantages of using a supported metal catalyst such as increased activity, surface area, and they are much cheaper than their bulk counterparts.[8, 9]

A supported metal catalyst is a dispersion of metal nanoparticles on a support.[10, 11] Only the exposed surface area of the metal nanoparticles is accessible for adsorption, constituting the active sites for a heterogeneous catalytic reaction.[12] For the development of such catalysts to enhance reaction rates, it is important to be able to quantify the actual amount of the exposed metal surface area in the catalyst. The number of active sites in a catalyst vary based on factors such as metal loading, type of support, geometry of the particles among others.[12] A one-dimensional schematic of a metal nanoparticle on a support with the exposed surface atoms highlighted, indicative of the active sites is illustrated in Figure 1. Adsorption of a species on the active sites may depend on its different configuration in the metal nanoparticle associated with terrace, step, edge, or kink positions. Certain reactions are structure insensitive such as olefin hydrogenation at high pressures (> 1 atm) meaning that all configurations active sites are identical for such

adsorptions. Structure sensitive reactions such as hydrogenolysis depend on the different configurations of the active sites.[13]

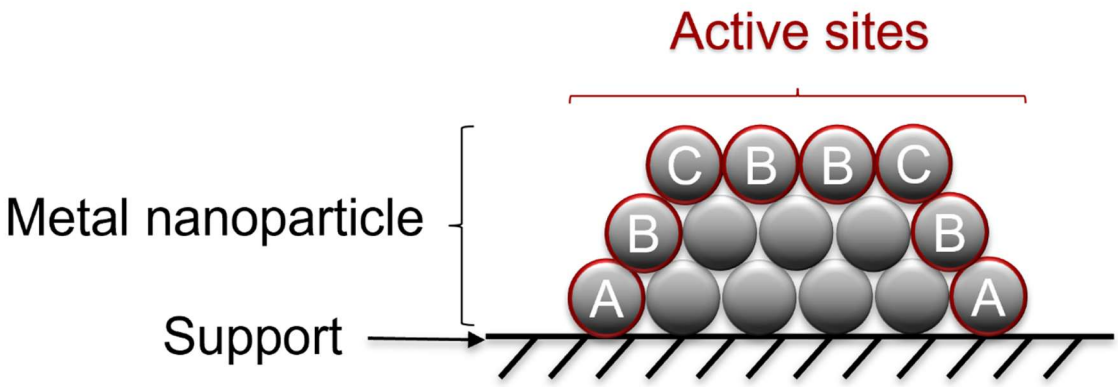

Figure 1: Schematic of metal nanoparticle on support. The atoms with red border are the surface atoms, indicative of the active sites. The letters A, B, and C indicate the different types of active sites based on the different configurations of atoms in the nanoparticle.

To obtain a standard for comparing catalysts, reaction rates are normalized with respect to the number of active sites.[14, 15] Turnover frequency (TOF) or site time yield (STY) are used as the normalized rates which are defined as the number of molecules reacting per active site per unit time.[16]

$$\text{TOF} = \frac{\text{Amount of product formed [mol]}}{\text{time [s]*amount of catalyst active sites [mol]}} \quad (1)$$

STY is used when all the active sites in a material are not identical and TOF is used otherwise.[17-20]

$$\text{STY} = \sum_i x_i \text{TOF}_i \quad (2)$$

x_i is the weighted fraction of the sites having the same activity and i is the number of different types of sites in a catalyst. Based on the illustration on Figure 1, the catalyst has three different types of active sites: A, B, and C.

Defined as the fraction of the exposed metal atoms in a supported catalyst,[15] dispersion allows us to estimate the TOF or STY.

$$\text{Dispersion} = \frac{\text{Number of surface metal atoms}}{\text{Total number of metal atoms}} \quad (3)$$

The dispersion for the catalyst illustrated in Figure 1 is 8/15 since there are a total of fifteen metal atoms in the catalyst out of which eight are on the surface.

Catalyst dispersion depends on the size and shape of metal nanoparticles. As the surface area to volume ratio decreases with increasing particle size, dispersion decreases.[21] The shape and size of nanoparticles depends on the technique used for synthesis of the supported metal catalysts. Nanoparticle size is also dependent on the metal loading on the support; higher metal loading results in larger nanoparticle sizes.[22] A survey of average platinum particle sizes in supported catalysts, synthesized using common techniques such as impregnation, deposition precipitation, and reductive deposition showed error bars larger than the particle sizes itself.[23] Thus, accurate catalyst dispersion cannot be estimated based on synthesis technique. Moreover, many studies are conducted using commercially available catalysts to understand kinetics of a reaction, their dispersion values are not reported by manufacturers.[24-26] These studies report conversion values on a specific catalyst instead of TOF or STY resulting in difficulty for comparison with other catalysts.

1.2 Background

Several catalyst characterization techniques can be used to get a dispersion estimate of the supported metal catalysts.[27, 28] Some techniques such as electron microscopy can determine the nanoparticle size and shape. Spectroscopic techniques have been extended to model the particle size distributions of metal nanoparticles. An estimation of the exposed surface atoms in a supported metal catalyst can also be obtained by analysis of chemical adsorption of probe molecules on the catalyst. The probe molecules are chosen as species which adsorb chemically on the metal and weakly on the support. The number of probe molecules chemisorbed on a given catalyst are estimated by techniques such as static chemisorption, pulsed chemisorption, or temperature-programmed desorption and correlated with the number of exposed surface metal atoms to get a dispersion estimate.

1.2.1 Transmission electron microscopy

Transmission electron microscopy is used to estimate the particle size and shape of the metal nanoparticle in a supported catalyst due to its high resolution.[29] The surface area of these nanoparticles is then estimated by geometry. The surface area can be translated to the moles of metal atoms on the surface of known atomic radius. Several studies use the transmission electron microscopy estimations of supported metal catalysts to determine their dispersion.[20, 30, 31]

There are several limitations to particle size estimation using transmission electron microscopy. Only a tiny fraction of the specimen is visible at a given time due to high magnification of the technique. Multiple images throughout the sample must be analyzed to ensure that the image is statistically representative of the sample. A transmission electron microscope gives a two-dimensional image of a three-dimensional specimen which could

be difficult to interpret accurately.[32] A high energy electron beam could damage the catalyst[33] resulting in inaccurate data interpretation. Moreover, catalyst characterization is done under ultra-high vacuum conditions which may not be an accurate representation of the catalytic surface at atmospheric conditions.[34, 35] A transmission electron microscope is an expensive equipment and requires special maintenance. Thus, it is only found in centralized facilities and is not easily accessible.[27]

1.2.2 Spectroscopic techniques

Spectroscopic techniques reveal information about the chemical composition of the sample.[36] This is exploited in catalysis to quantify the amount of surface covered by metal active sites.

X-ray photoelectron spectroscopy works on the principle of photoelectric effect where the incident photon radiation results in emission of an electron from the sample. The kinetic energy of this electron is measured, and its binding energy is estimated from the instrument parameters. The binding energy of the electron in the sample reveals information about the surface chemical composition. The percentage of metal in the catalyst can be quantified using the peak intensities obtained by X-ray photoelectron spectroscopy.[37, 38] Several models have been developed to estimate the dispersion of supported metal catalysts from the intensity information obtained from X-ray photoelectron spectroscopy.[38]

Kerkhof and Moulijn[39] have developed a model to estimate the particle sizes of supported metal nanoparticles using the peak intensities from X-ray photoelectron spectroscopy and demonstrated their accuracy for platinum supported on silica catalysts. Their model relates the intensities of promoter (metal) and the support to the non-

dimensional parameter (α_1) which is the ratio of the dimension of cubic crystallites to the escape depth of the electrons traveling from the promoter through the promoter. The intensities are estimated from the principles of X-ray photoelectron spectroscopy, and the escape depth is known. Thus, the dimension of the particle can be estimated. This model is valid only for homogeneous distribution of the particles on high area supports.

The Davis model[40] proposes the particle size estimation of a cube using X-ray photoelectron spectroscopy principles using the intensity ratios for emission of electrons from two dispersed phase core levels which have a different kinetic energy, the photoionization cross-section , the attenuation wavelength , and the instrumental factor. Based on the particle shape, the model uses an attenuation factor for an accurate estimation of the particle size.

A comparison of particle sizes estimates using the above mentioned models and transmission electron microscopy for supported palladium catalysts was studied to determine their efficacies.[38] Both models showed good agreements with transmission electron microscopy measurements for lower particle sizes, but large discrepancies were observed as particle sizes increased. Thus, theoretical models need to be expanded to give a reliable universal estimate of particle sizes of supported metal catalysts. Moreover, the instrumentation for X-ray photoelectron spectroscopy is usually located in centralized facilities due to the high cost of the instrument and sensitivity due to vacuum atmosphere making it difficult to access.

X-ray absorption spectroscopy has also been exploited for particle size estimations of supported metal catalysts. It is based on the principle of electron removal from core levels of sample when exposed to x-rays.[41] This technique does not require vacuum

conditions unlike X-ray photoelectron spectroscopy.[37] A type of X-ray absorption spectroscopy, extended X-ray absorption fine structure (EXAFS) is used to study the local characteristics of the sample such as co-ordination number and distance between atoms. EXAFS is the X-ray absorption spectroscopy at energies greater than the threshold for electron release from the sample such that the electron is back-scattered by the electron shells in the sample.[41]

De Graaf et al.,[42] studied particle size estimation of platinum supported on zeolite using EXAFS. They proposed a model that related first shell co-ordination number of platinum particles per size [$N_{Pt\text{-}Pt}$] to the platinum molecular weight [MW_{Pt}], Avogadro's number [N_A], platinum loading [$Pt_{loading}$], number of platinum particles per size per gram catalyst [$\frac{P}{g_{zeolite}}(size)$], and the number of platinum atoms per particle size [$A(size)$] as shown in equation (4)

$$N_{Pt\text{-}Pt} = \frac{MW_{Pt}}{N_A * Pt_{loading}} \int_{size=0}^{\infty} \frac{P}{g_{zeolite}}(size) * A(size) * N_{Pt\text{-}Pt}(size) \quad (4)$$

This model works only if the particle size distribution is narrow, and the particle size is small. Particle size distribution using EXAFS is not extensively studied yet and hence, it cannot be used as a standalone technique for dispersion estimation.[42] Like X-ray photoelectron spectroscopy, EXAFS instruments are also usually only located in centralized facilities making them not easily accessible.

1.2.3 Chemisorption

Chemisorption is commonly employed for measuring the exposed metal surface area due to its relative inexpensiveness, ease of access, and simple operation.[43, 44]

Moreover, in certain studies, it has been reported that chemisorption gives a more reliable dispersion estimation compared to electron microscopy.[20, 31]

Chemisorption is based on the principle that probe molecules chemically adsorb on the metal surface but do not adsorb or weakly adsorb on the inert support. The amount of probe molecules adsorbed can be used to estimate the dispersion by knowing the stoichiometry ratio of the adsorbate and adsorbent.[43] Carbon monoxide (CO) is a commonly used probe molecule for chemisorption on platinum group metals.[43, 45]

There are two approaches through which catalyst dispersion can be estimated isothermally using chemisorption: static and dynamic.

In static chemisorption, the moles of CO adsorbed on the metal surface are estimated through a series of measured adsorption isotherms. During the first adsorption isotherm, the CO molecules adsorb on the metal surface as well as on the support. The molecules on the support are reversibly adsorbed while the molecules on the metal are irreversibly adsorbed. The catalyst is then subjected to vacuum to allow desorption of reversibly adsorbed molecules. This is followed by measuring another isotherm at the same conditions as the first one but now the surface already is populated with irreversibly adsorbed species. The difference between the consecutive isotherms is associated with the irreversibly adsorbed molecules, which are representative of the exposed metal surface area and thus, can be used for dispersion estimation.[44] Static chemisorption technique requires vacuum of at least 10^{-4} torr resulting in higher instrumentation costs.[45]

In isothermal dynamic chemisorption (known as pulse chemisorption), pulses of a stream of CO are passed through the catalyst. The amount of CO pulsed should be less than the moles of exposed metal atoms. During initial pulses, all CO molecules are adsorbed on

the metal surface. Once the catalyst surface is saturated with CO, excess CO is detected in the effluent from the catalyst bed. The difference between the moles of CO pulsed and those detected in the effluent is equal to moles of CO adsorbed on the catalyst surface, which can be used to estimate dispersion.[45] The dynamic approach can be implemented at near ambient conditions, and hence, it is widely used to estimate the dispersion of metal catalysts.[45]

Dynamic chemisorption is often coupled with temperature-programmed desorption analysis. CO is pulsed into the catalyst bed such that the surface is saturated. After saturation, the catalyst is subjected to a stream of inert gas and its temperature is ramped linearly to obtain the desorption profile of CO. The system is coupled with a detector such as a mass spectrometer to quantify the amount of CO desorbed. From the desorption profile of CO with temperature, the amount of CO that was adsorbed on the catalyst can be estimated.[45]

Catalyst dispersion using chemisorption is typically estimated using the commercially available instruments.[46-50] Commercial instruments measure the dispersion of the catalyst using static or dynamic chemisorption techniques and temperature-programmed desorption. A thermal conductivity detector is typically used to quantify the desorbed gases. However, commercial instruments are expensive and thus could be inaccessible to use in many research laboratories.

Karakaya and Deutschmann[47] identified the need for an inexpensive and readily accessible dispersion estimation technique for commercial catalysts. They suggested a technique based on chemisorption using temperature programmed desorption (TPD) and mass spectroscopy. They showed that their dispersion measurements agreed well with the

measurements using commercial instruments for a diesel oxidation catalyst based on platinum on alumina. However, they detected considerable carbon dioxide desorption during the chemisorption and by process of elimination, concluded that carbon dioxide is a result of CO oxidation due to impurities in the carrier gas. Thus, their dispersion measurements assumed that both desorbed species (carbon dioxide and CO) result from CO and no disproportionation reaction takes place. This assumption might be true for the one catalyst tested but potential complications could arise on different catalysts due to structure sensitive phenomena. For example, Souza and Schmal[51] concluded that the deactivation of platinum on alumina catalyst used in their study was due to the CO disproportionation reaction to form carbon dioxide and coke, and Pramhaas et al.,[52] reported that CO disproportionation occurs at low coordinated platinum sites at high CO coverage. Foger and Anderson[53] reported carbon dioxide from a catalyzed reaction between CO and hydroxyl ions in the support on platinum/γ-alumina. Hence, the presence of carbon dioxide and lack of samples of catalysts tested indicate that the reliability of the technique proposed is yet to be demonstrated.

In conclusion, spectroscopic techniques coupled with theoretical mathematical models can be used for dispersion estimation for a certain range of particle sizes of metals dispersed on supports but need further validation to be used universally. The high cost and maintenance requirements of the equipment restrict their accessibility. Transmission electron microscopy is commonly used for dispersion estimation but is limited by inaccurate data representation due to small sample size, vacuum conditions, and possibility of damage from high electron beam. The transmission electron microscope is usually only available in centralized facilities and hence, difficult to access. Thus, commercial

instruments for dispersion estimation rely on chemisorption measurements due to their relatively high reliability and simple operation. However, the high cost of these instruments may hinder their use, prohibiting several researchers to report reaction rates as TOF or STY. Thus, an inexpensive, easily accessible, and reliable dispersion measurement tool would be an asset to catalysis research.

1.3 Objectives

The overarching goal is to develop a reliable experimental technique for dispersion estimation using readily available tools and equipment in a catalysis focused research laboratory. A simple technique to measure the dispersion of platinum group metal supported catalysts using a gas chromatograph via dynamic pulse CO chemisorption technique is proposed. A gas chromatograph is common to catalysis laboratories and no additional reactor set-up or analytical instrument is required. The desired applicability of this technique ranges from varying metal weight loadings and support identities. Dispersion values for catalyst samples known from commercially available equipment were used to test the efficacy of this technique. This would provide researchers with an accessible analytical tool to estimate the exposed surface area of the supported metal catalysts allowing for reporting standardized reaction rates in terms of TOF or STY. A strategy for complete automation of this technique is also devised.

The cost for setting up chromatographic dynamic chemisorption on an available gas chromatograph is lower by an order of magnitude than the commercially available instruments. Moreover, the gas chromatograph used for the set up need not be dedicated to conducting dynamic chemisorption experiments but can be used interchangeably with other applications.

Moreover, commercial dynamic chemisorption instruments are usually equipped with a thermal conductivity detector (TCD) to quantify the CO exiting the catalyst bed. A TCD cannot distinguish between CO and carbon dioxide. Thus, any oxygen impurity which might result in carbon dioxide formation during chemisorption could go unnoticed and result in inaccuracy of dispersion estimated. An oxygen impurity might be found in the carrier gas and thus, needs to be confirmed. A gas chromatograph with a column separates CO from carbon dioxide and detects it resulting in a check that the system is free of oxygen. This is an added advantage of using chromatographic dynamic chemisorption over commercial instruments.

CHAPTER 2

MATERIALS AND METHODS

2.1 Materials

2.1.1 Catalyst Samples

The supported metal catalysts used were: 1 weight % (wt%) platinum on silica (Sigma Aldrich, 520691), 1 wt% platinum on alumina (Sigma Aldrich, 232114), 0.5 wt% platinum on alumina (Micromeritics 004/16825/00), 5 wt% platinum on carbon (Strem Chemicals, 78-1509), 2 wt% ruthenium on alumina (Alfa Aesar, 44575) and, 5 wt% palladium on carbon (Strem Chemicals, 46-1709). MCM-41 silica (ACS Materials, MSM41A01) and chloroplatinic acid hexahydrate (Sigma Aldrich, 206083) solution in water (Resistivity > 18.2 MΩ) from an in-house purifier were used for synthesis of 0.12 wt% platinum on silica catalyst via incipient wetness impregnation.[54] A 62.5 ml solution of 46.5 mg chloroplatinic acid in water was prepared and 4.2 ml of this solution was added to 1.0 g of MCM-41 silica support. The catalyst was allowed to dry overnight at 353 K. Once dried, the catalyst was reduced in 100 sccm hydrogen for 4 hours at 673 K at a ramp rate of 3 K min^{-1}. After reduction, the catalyst was passivated in 10% (by volume) air in helium for 5 minutes at room temperature (298 K).

2.1.2. Gases

Hydrogen (Airgas, 99.999% purity) was used for pre-treatment of the catalysts and nitrogen (Airgas, 99.999% purity) was used as a carrier gas as well as to blend with pure CO (Airgas, 99.5% purity) for pulsing. A 1% CO (Airgas, 99.99% purity) in helium (Airgas, 99.99% purity) blend was also used for pulsing in some cases.

2.2 Experimental set-up

A gas chromatograph (Agilent 7890B) equipped with a HP-PLOT Q (Agilent, 19091P-QO4) column and flame ionization detector (FID)/methanizer (Jetanizer, Activated Research Company) with minimal modifications was used for dispersion estimation as shown in the schematic in Figure 2a. A splitless quartz inlet liner of inner diameter 4mm (Agilent, 5190-3162) was used to pack the catalyst bed, sandwiched between quartz wool (Restek 24324) and was inserted into the inlet of the gas chromatograph. An air actuated 6-port valve (Valco) equipped with a sample loop (47 μL or 250 μL, depending on the application) was used to pulse CO into the packed bed as depicted in Figure 2b and c. To ensure that the amount of CO pulsed during each pulse was less than the amount required to saturate the catalyst surface, a CO blend with inert gas and a sample loop with a volume in the microliter range was used. The 6-port valve was set-up such that when CO was not pulsed through the system, carrier gas flowed through the catalyst bed. The carrier gas was varied between hydrogen used during the pre-treatment and nitrogen used during pulsing, using an air actuated 4-port valve (Valco). The outlet of the inlet liner was connected to the column and the split vent. Flow through the column was set at constant linear velocity of 20 cm/s and remaining gas was ejected through the split vent. The ability of the column to separate the gases served as a check for any impurities present in the system. The gas flowing through the column was detected using the FID coupled with a methanizer. A FID cannot be used by itself because it is only responsive to compounds containing both carbon and hydrogen.[55] The methanizer converts CO to methane which can be detected by the FID.

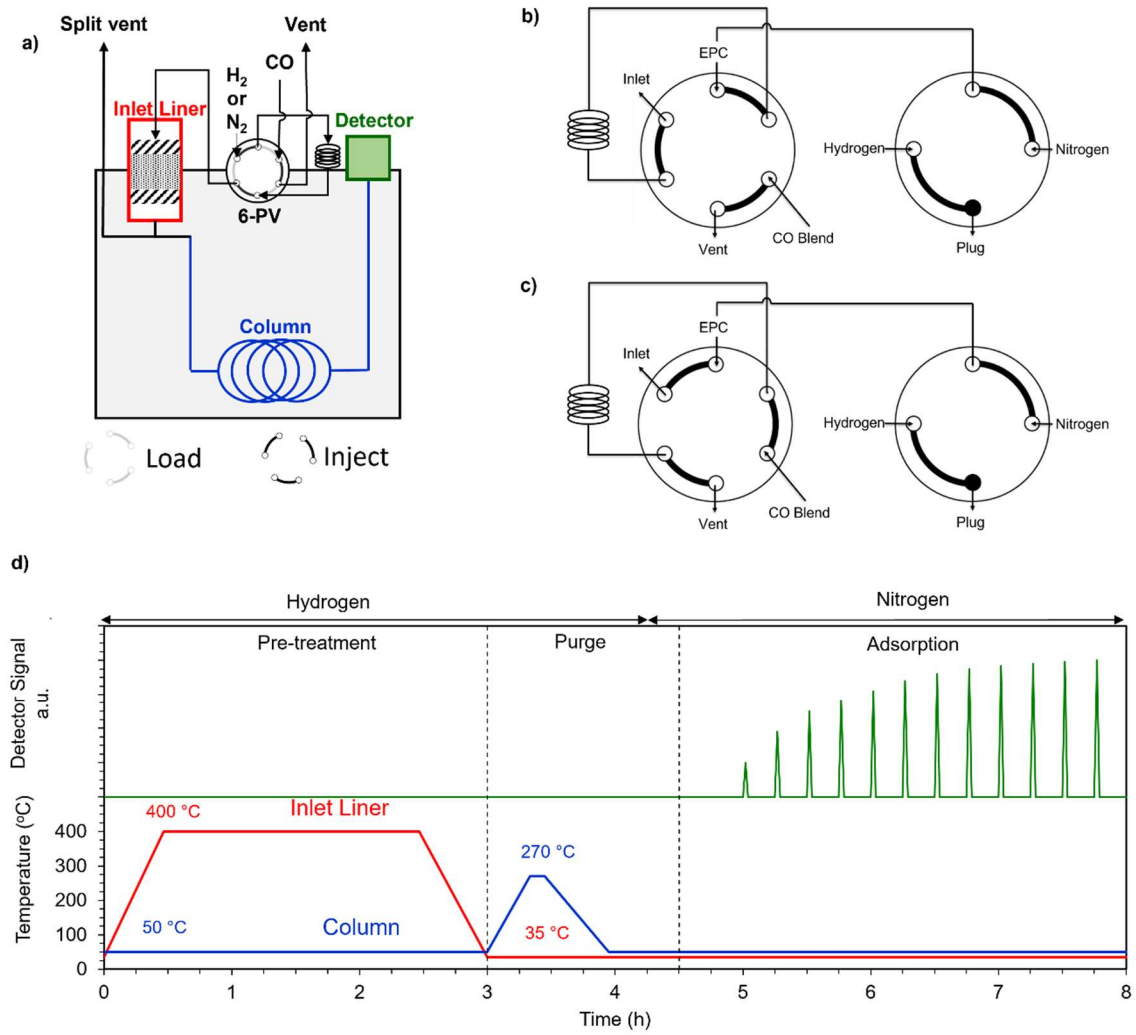

Figure 2: a) Schematic of gas chromatograph with flow paths during CO pulsing b) Gas flow paths through 6-port valve (6-PV) during inject position. c) Gas flow path through 6-PV during load position. Nitrogen gas flows through the electronic pneumatic control (EPC) of the gas chromatograph during both load and inject positions whereas hydrogen gas is used during pre-treatment and the position of the 4-port valve is switched. d) Dispersion estimation method sequence: (1) Pre-treatment in hydrogen at inlet liner temperature of 400 °C, (2) Column purge in hydrogen while its temperature is ramped to 270 °C followed by nitrogen purge of entire system at operating temperatures, and (3) Isothermal CO pulsing.

2.3 Method

Dispersion estimation of platinum group supported metal catalysts using a gas chromatograph by CO pulse chemisorption technique is illustrated in the schematic in

Figure 2. Figures 2a, b, and c show the gas flow paths on the system to facilitate pre-treatment in hydrogen, purge in nitrogen and CO pulsing. Figure 2d shows the conditions at which the pre-treatment, purge and CO pulse chemisorption is carried out by an automated sequence in the gas chromatograph. The details of each method have been described in the following sections.

2.3.1 Catalyst preparation

The commercial 1 wt% platinum on silica catalyst pellets were crushed and sieved to 1 - 1.4 mm in average diameter. Catalyst samples were calcined ex-situ in air at 450 ^{o}C for 1 hour at 5 ^{o}C min^{-1}. In case of 1 wt% platinum on alumina, 0.5 wt% platinum on alumina, and, 2 wt% ruthenium on alumina samples, the 3 mm pellets were finely crushed using mortar and pestle (VWR) before loading. The 5 wt% platinum on carbon, 5 wt% palladium on carbon, and 0.12 wt% platinum on silica catalysts were used as is.

A known mass of catalyst was sandwiched between two plugs of quartz wool (Restek, 24324) in the inlet liner. Quartz wool was added such that the catalyst bed was located between 20 - 50 mm from the bottom of the inlet liner, to ensure there was no temperature change within the length of the bed and to ensure an accurate temperature, with a minimal gradient along the length of the bed.(<5 K)[56] The inlet liner was then placed in the inlet of the GC. All measurements were performed at catalyst temperature of 35 ^{o}C and GC oven temperature of 50 ^{o}C unless specified.

2.3.2 Pre-treatment

All catalysts were pre-treated in-situ at 400 ^{o}C in 50 sccm of hydrogen for two hours, then cooled to the desired adsorption temperature, while maintaining the chromatography column temperature at 50 ^{o}C.

2.3.3. Purge

After the catalyst pre-treatment, the oven temperature was ramped to 270 ^{o}C at 10 ^{o}C min^{-1} and held for eight minutes, then cooled back to 50 ^{o}C. 'This was performed to elute any compounds retained in the chromatography column. The front inlet temperature rose to about 75 ^{o}C while heating up the column due to heat transfer effects since the front inlet and the column are not completely insulated from each other in a gas chromatograph. Since the rate of increase and cooling down of the front inlet temperature is not controlled in this scenario, time required for the front inlet to cool to its desired temperature solely depended on the environmental conditions. The variability in time exposure of catalyst to nitrogen was undesirable due to the possibility of oxygen contamination in prolonged conditions. Thus, the catalyst was continued to be purged in hydrogen while the column and front inlet cooled down to their desired temperatures. Once, the gas chromatograph components attained their desired temperatures, the gas supply was switched to nitrogen to purge the hydrogen from the system for twelve minutes. Nitrogen was used as an inert carrier gas during pulsing.

2.3.4. CO pulse chemisorption

A stream of pure CO was mixed with nitrogen to generate a 3.1% (by moles) blend which was passed through a 47 μL sample loop (0.01" ID, 1/16” OD, 316 stainless steel capillary tubing, Restek) on the six-port valve. The CO blend was pulsed through the catalyst bed every seven minutes. Pulsing was continued until the moles of CO detected did not vary in ten consecutive pulses indicating that all the active sites on the catalyst were saturated with CO. This procedure was carried out to measure several dispersion values for platinum on silica catalyst.

For the remaining measurements, a pre-mixed 1% (by moles) CO blend in helium was used and this was passed through a sample loop (Valco) having a volume of 250 μL and pulsed in the same manner as described above. The flow rates of gases were controlled using mass flow controllers. (Brooks 5850S)

2.4 Automation

Methods for pre-treatment, purge and adsorption were set up on Chemstation software linked with the gas chromatograph. Air actuators (Valco) that can be controlled using the gas chromatograph were used to switch the carrier gases from hydrogen to nitrogen as indicated in Figure 2. This valve switching mechanism was incorporated in the methods ensuring that the valve position would switch at the desired time to change the carrier gas. The methods controlled the flow through column, the temperatures of the inlet liner and the column, the valve position, and the time duration. A sequence of methods was designed such that the conditions would change from pre-treatment to purge to adsorption as depicted in Figure 2. This ensured that once the catalyst bed was loaded and the sequence was run, the entire procedure from pre-treatment to adsorption would occur without any intervention.

2.5 Dispersion estimation

Using the experimental set-up described in Section 2.2 and the methods described in Section 2.3, a breakthrough profile of CO adsorption on 1 wt% platinum on silica catalyst was obtained as shown in Figure 3. From this breakthrough profile, the total moles of CO adsorbed were determined by obtaining a difference between the total moles of CO pulsed into the liner and the total moles of CO that did not adsorb and were detected at the exit of the liner. The moles of CO detected at the outlet after each pulse were quantified by

the areas of peaks of the respective pulses. It was assumed that the area corresponding to the CO peak was equivalent to the number of moles of CO pulsed, once the breakthrough profile showed saturation. The moles of CO pulsed were estimated using the ideal gas law where the loop volume, and mole fraction of CO in the blend was known; the temperature at the surface of the loop was measured; and the atmospheric pressure with the added pressure drop across the sample loop and the 6-port valve was measured and accounted for while estimating the number of moles of CO pulsed. A calibration factor was determined based on the moles of CO pulsed and the area of peak detected after saturation of the catalyst bed. A unique calibration factor for each run was calculated based on the peak saturation area for that catalyst. This was because changes in the catalyst bed (mass, length of the bed, particle size) resulted in variation in pressure drop across different beds causing a change in the split ratio (flow to the split vent/total gas flow). This led to a change in the amount of CO passing through the column and reaching the detector for each different bed used, resulting in a change in the calibration factor.

For each pulse, a difference between the area of peak of CO detected and the stabilized area of peak of CO at catalyst saturation was calculated to quantify adsorption during each pulse. The sum of the areas representing adsorption in each pulse was calculated and the moles of adsorbed CO was estimated by multiplying it by the calibration factor. The stabilized peak area of CO at catalyst saturation was taken as the average of the areas corresponding to the last ten CO pulses through the catalyst bed. The moles of adsorbed CO were correlated to the exposed metal surface area of the catalyst by the stoichiometry factor. The stoichiometry factor (CO : Metal) of CO on platinum and ruthenium was taken as one and for CO on palladium was taken as 0.6.[45] Multiplying the

adsorbed moles of CO with the stoichiometry factor gave the moles of exposed metal surface. The total moles of metal in the bed were estimated from the known metal loading and the mass of catalyst loaded. Dispersion was calculated as the ratio of the exposed moles of metal to the total moles metal in the catalyst loaded in the bed. The calculations are shown by equations, (5) and (6).

$$\text{Total nanomoles of CO adsorbed} = \sum(\text{nanomoles of CO fed -nanomoles of CO detected}) \quad (5)$$

$$\text{Dispersion} = \frac{\text{Total nanomoles of CO adsorbed}}{\text{Total nanomoles of Platinum in catalyst bed}} \quad (6)$$

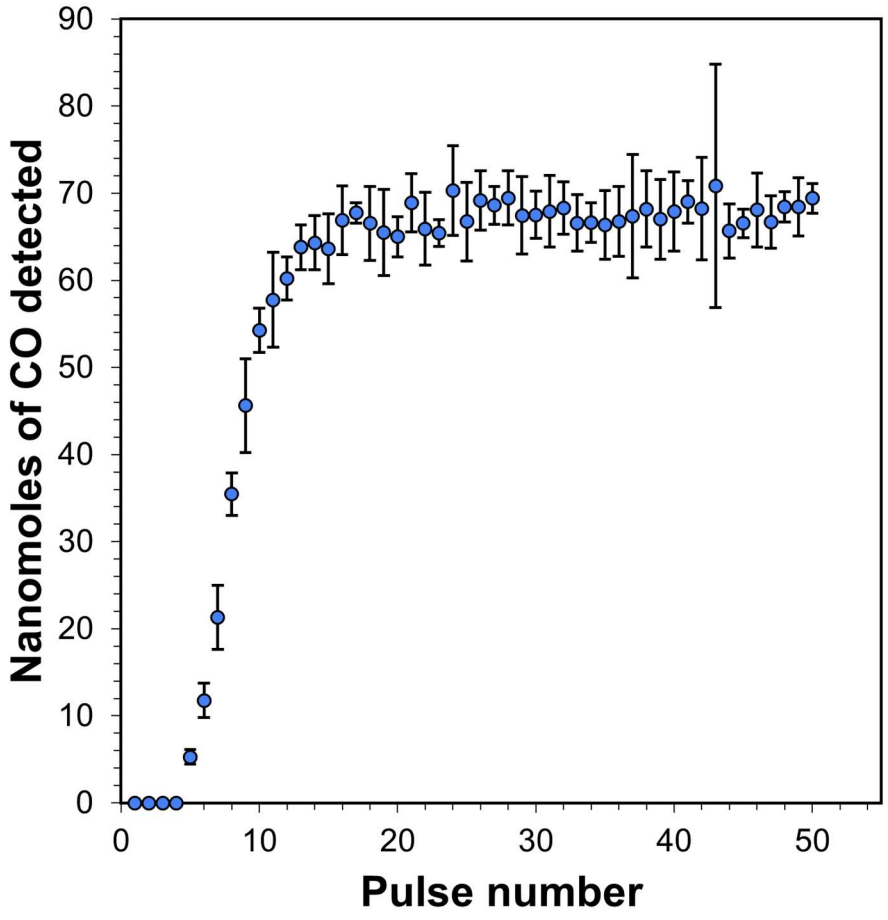

Figure 3: Breakthrough profile for 1 wt% platinum on silica catalyst at 35 ºC

2.6 Error estimation

The flame ionization detector is popularly used in gas chromatography applications due to its low detection limits in the range of 10^{-12} gs^{-1} and an extremely linear response range over six orders of magnitude.[57] The errors due to the response factors of the gas chromatograph are negligible in comparison to errors introduced due to instrumental fluctuations.[58] Thus, the errors in this study are reported as precision errors calculated from multiple measurements of the same type.

To estimate the dispersion of a particular supported metal catalyst, the catalyst bed was pre-treated, purged, and adsorption measurements were conducted to obtain a breakthrough profile. After the breakthrough profile was obtained, the same bed was pre-treated again for reactivation, and adsorption measurements were carried out without removing it from the gas chromatograph inlet. Five such repetitions were carried out to estimate the dispersion, and the average value and standard deviation were reported. The absolute error was calculated at 95 % confidence intervals using the student t-test for the estimate. The average value across the five repetitions with an absolute error value calculated is reported for each dispersion measurement as:

$$\text{Absolute error} = \frac{s * t_{0.05/2,\nu}}{\sqrt{n-1}} \tag{7}$$

where s is the standard deviation, $t_{0.05/2,\nu}$ is the value corresponding to 95% confidence interval and ν degrees of freedom, obtained from the student t-test table and n is the total number of repetitions.

CHAPTER 3

RESULTS AND DISCUSSION

3.1 Dispersion estimations using 3.1% CO in nitrogen blend and 1% CO in helium pre-mixed blend

Several experiments for dispersion estimation of 1 wt % platinum on silica catalyst were conducted by using pure CO and blending it with nitrogen to produce a 3.1 % (by moles) CO in nitrogen blend. This is an economical choice over pre-blend mixes but posed several practical challenges.

To ensure that the mole fraction of CO in the blend was <5%, high flow rates of nitrogen gas were used which resulted in a high total flow rate of the blend through the capillary loop and the six-port valve causing a high pressure drop. The pressure drop was measured using a pressure gauge on the gas line containing the CO in nitrogen blend entering the six-port valve. The gauge measured the pressure drop across two micro channels of the six-port valve and capillary loop through which the gas passed before venting into the atmosphere as shown in the flow paths in Figure 2. The total flow rate of the gas across the sample loop of inner diameter 0.01 inches and the 6-port valve was 100 ml min^{-1}. Due to friction between gas and the walls of the capillary channels, a significant pressure drop was observed which varied across the length of the capillary loop.[59] To estimate the moles of CO in each pulse, using the ideal gas law, the variation of pressure-drop across the length of the capillary loop needed to be accounted for. The pressure gauge measured the total pressure drop across the flow path of the gas but did not show variation of pressure drop along the path. It was established that the major contribution of pressure drop in the flow path was the microchannels in the 6-port valve and the sample loop by

observing the total pressure drop on the gauge bypassing these two flow components. To accurately estimate the moles of CO in the loop, an average pressure drop value across the loop was required instead of the pressure drop at the beginning or the end of the loop. The variation of pressure drop across a pipe is not linear, thus eliminating the possibility of determining the average value by interpolation. Thus, a pressure multiplier factor was estimated as the ratio of areas of CO detected due to pressure drops at high flow rate to the area detected at negligible pressure drop by using a low flow rate of the pure CO tank. Since, the same flow path was used in both cases, it was assumed that the high flow rate was the major contribution to the observed pressure drop. A pressure multiplier factor was calculated to be 1.48 which was incorporated in the calculation of moles of CO using the ideal gas law.

Comparison of dispersion estimates using the pressure drop correction and the 3.1 % CO in nitrogen blend with 1 % CO in helium pre-blend with negligible pressure drop showed comparable results over 95 % confidence intervals. Dispersion of about 50 mg of 1 wt % platinum on silica using 3.1 % CO in nitrogen blend was (27 ± 2) % whereas measurement using 1 % CO in helium pre-mixed blend was (25 ± 2) %.

3.2 Selection of carrier gas and purge duration

Platinum group metals are known to oxidize on exposure to air. Hence, their pre-treatment is usually a reduction in hydrogen at high temperatures.[17] The CO pulsed chemisorption is not carried out in presence of hydrogen carrier gas since hydrogen adsorbs on platinum group metals and it might interfere with the CO adsorption. The amount of CO chemisorption on platinum saturated with hydrogen is reported to be two-thirds of the

amount of CO chemisorbed on a clean platinum surface.[60, 61] Thus, an inert carrier gas such as nitrogen is used during chemisorption measurements.

The inert carrier gas usually contains a minor amount of oxygen impurity. Oxygen chemisorbs on the platinum surface as atomic oxygen. This might result in blocking the active sites for carbon monoxide adsorption. Also, the atomic oxygen reacts with adsorbed carbon monoxide to form carbon dioxide in presence of platinum group metals.[62] Thus, oxygen impurity over a certain threshold in the CO chemisorption system can result in carbon dioxide formation which interferes with accuracy of dispersion measurements.[47] The gas chromatography column can separate CO and carbon dioxide and hence, serves as a check for oxygen impurities.

It was observed that purge times greater than thirty minutes in nitrogen resulted in sufficient amount of oxygen dissociatively adsorbing on the platinum surface and reacting with CO to form carbon dioxide. Thus, the technique was optimized to ensure that column purging takes place in the presence of hydrogen after which only a few minutes of nitrogen purge is done to ensure removal of any hydrogen molecules from the system before pulsing starts. No carbon dioxide peaks were observed when the purging time in nitrogen was set to twelve minutes. Thus, it was ensured that all dispersion measurements were accurate and not contaminated by the presence of atomic oxygen adsorbed on the metal surface.

3.3 Non-idealities in a packed bed

The catalyst filled in an inlet liner is a packed bed. Thus, all the non-idealities associated with a packed bed need to be accounted for, to accurately estimate the dispersion of the metal catalysts. In a fixed packed bed reactor, gases may undergo channeling or bypassing, deviating from their plug flow behavior resulting in ineffective contact between

the adsorbent and the catalyst.[63] These effects were observed when the physical properties of the catalyst in the bed were changed. The shape of the breakthrough profile varied largely as shown in Figure 4 when a crushed catalyst pellet was used as opposed to a whole 3 mm pellet of 1 wt % platinum on alumina catalyst. Since the inner diameter of the inlet liner is 4 mm and the pellet size is 3 mm, it is possible that bypass effects resulted in a non-ideal breakthrough curve. Comparing the breakthrough curves in both cases in Figure 4, the nanomoles of CO detected when the pellet is finely crushed stabilize after ten pulses as opposed to the case where the whole pellet is used and nanomoles of CO detected stabilize after 38 pulses. The small adsorption of CO in each pulse for 38 pulses when a whole pellet is used versus complete adsorption of CO in the first six pulses followed by a sharp increase and stabilization after ten pulses when finely crushed pellet is used could be an indication that all the CO that passes through the packed bed does not effectively contact the catalyst when a whole pellet is used. This could result in the breakthrough profile as shown in Figure 4 for the whole pellet that the catalyst takes a greater number of pulses to saturate and there is no complete adsorption during the initial pulses since some amount of CO bypasses the catalyst.

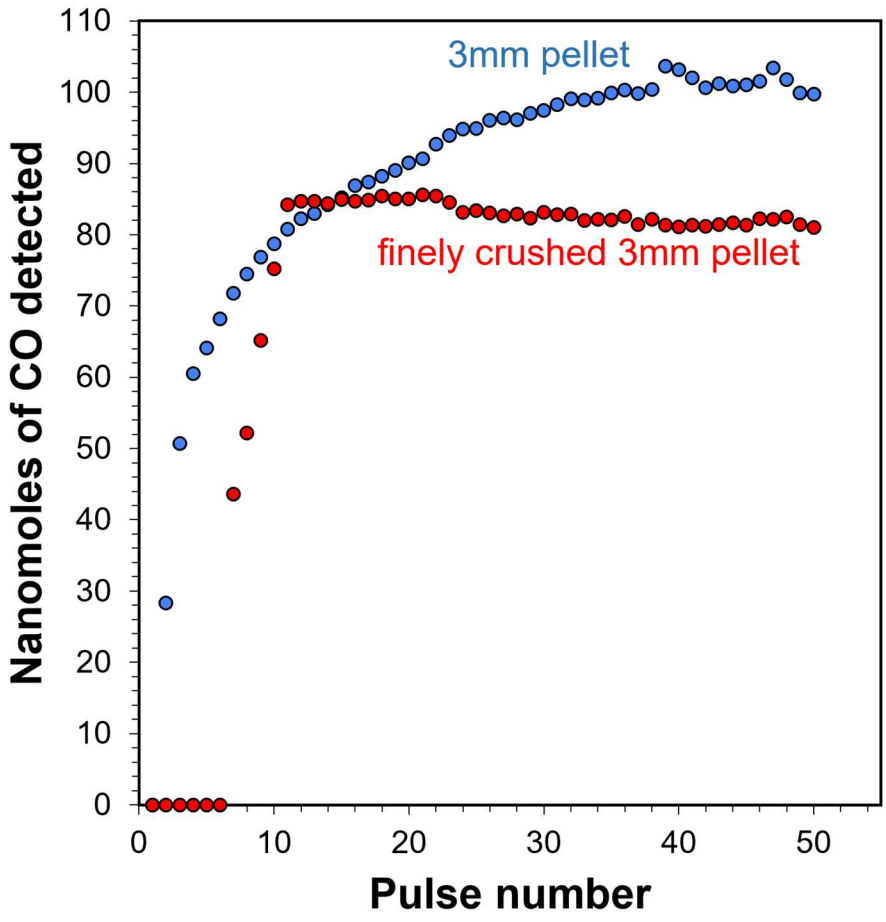

Figure 4: Breakthrough profile variation with catalyst particle size for the same catalyst mass in case of 1 wt% platinum on alumina catalyst. The total amount of CO adsorbed per mass of catalyst was13 nmol/mg in case of 3mm catalyst pellet and 15 nmol/mg in case of finely crushed catalyst pellet. The error bars for the breakthrough profiles are not indicated since the figure serves to highlight the difference in shape of the breakthrough profiles and statistically sufficient measurements for error analysis were not obtained at these conditions.

Another effect of changing particle size is the variation of pressure drop across the catalyst bed. Varying catalyst mass also affects the pressure drop across the bed since the length of the packed bed increases with increased catalyst mass. Changing pressure drop in the catalyst bed results in a change in the split ratio of the gas since the opening of the split vent valve is pressure controlled. Thus, the amount of gas flowing through the column

into the detector varies with varying pressure drop across the bed. Hence, each time the catalyst bed is changed, a unique calibration factor needs to be estimated to relate the area of peak of CO detected to the moles of CO pulsed. The moles of CO pulsed are same in each case, but the detector signal varies since the moles of CO reaching the detector vary in each case due to unequal distribution of gas through the split vent and the column. From the breakthrough profiles in Figure 4, it is observed that for the catalyst pellet of larger size, the pressured drop across the liner would be low which would lead to increased flow through the column and hence, the amount of CO reaching the detector is more than in case of catalyst with smaller particle size. This is corrected by relating the average saturation peak areas of the last ten pulses to known amount of CO pulsed for each change in catalyst bed to get an accurate estimate of the moles of CO adsorbed.

Besides, for all catalysts, the breakthrough profile was observed and necessary variations in catalyst particle sizes were made to minimize any bypassing or channeling effects. A sharp S-shaped breakthrough profile is indicative of effective contact between the catalyst and adsorbent since complete adsorption occurs during the initial pulses followed by catalyst saturation. In absence of non-idealities such as channeling or diffusion limitations, the breakthrough profile is representative of instantaneous mass transfer of the adsorbent from the gas stream to the catalyst surface.[64] Presence of bypassing and channeling in the packed bed prohibits effective contact between the adsorbent in the gas stream and the catalyst. Besides, increased number of pulses between the region of complete adsorption and saturation results in an increased total number of pulses required for dispersion estimation via chemisorption. The total moles of CO adsorbed are calculated as the sum of CO adsorbed in each pulse which has an error associated with it. Thus,

increased total number of pulses would result in the summed increase in error in estimating total CO moles adsorbed and hence, dispersion. Hence, optimization of parameters such as catalyst mass, catalyst size, amount of CO in each pulse was conducted to ensure maximum resemblance of the breakthrough profile with the ideal S-shaped curve.

3.4 Dispersion variation with catalyst bed temperature

Dispersion values for 1 wt% platinum on silica at 35 ^{o}C and 50 ^{o}C were measured, covering the range of temperatures at which pulsed chemisorption experiments are typically carried out. CO weakly adsorbs on the support but chemically adsorbs on the metal surface. Weak adsorption is a strong function of the temperature at which adsorption occurs, but chemisorption is associated with highly exothermic heats of adsorption which do not depend on temperature. Thus, estimated dispersion values would vary significantly with changes in temperature if CO was weakly adsorbing on the support during dynamic chemisorption measurements. As shown in Figure 5, the measurements did not show any effect of temperature change corroborating the fact that CO pulse chemisorption was representative only of the metal active sites and not the support.

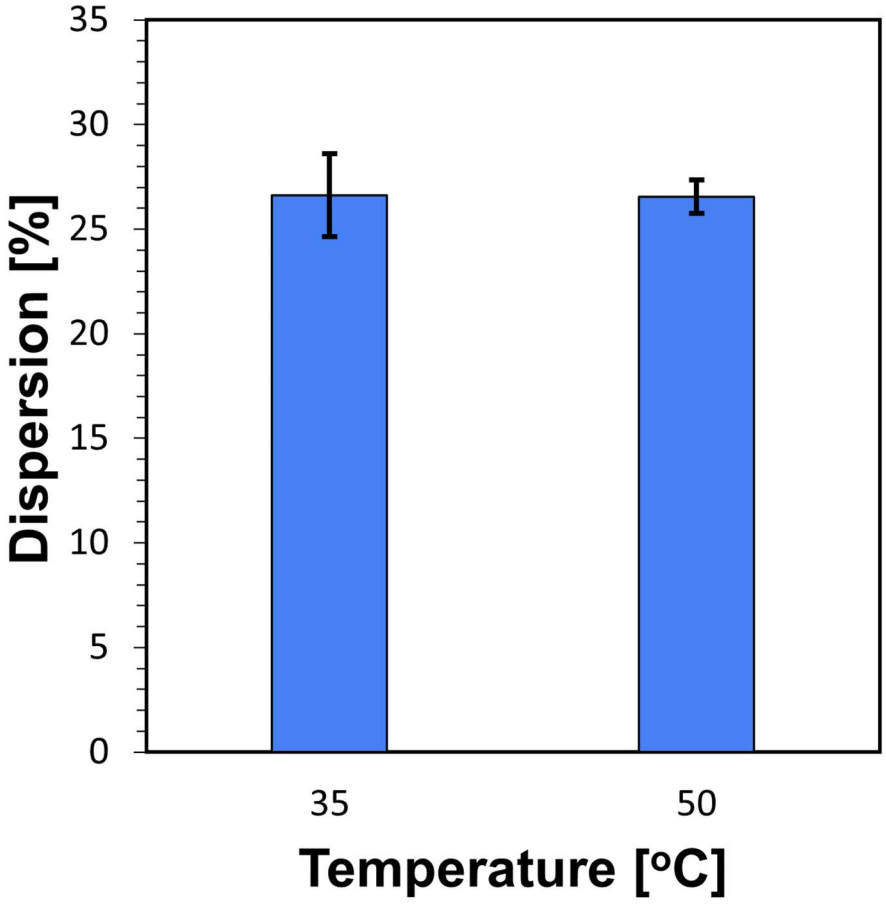

Figure 5: Dispersion of 1 wt % platinum on silica at 35 °C and 50 °C.

3.5 Dispersion variation with catalyst mass

Dispersion is an intensive quantity and should therefore not depend on the mass of catalyst in the packed bed. The dispersion values measured for 1wt% platinum on silica catalyst at 35 °C with masses varying from 19 mg to 99 mg were constant as shown in Figure 6 to give an average dispersion of 29 %. Thus, the proposed technique of measuring dispersion using a GC shows reproducible results with variation in mass as one would expect an intensive quantity to show.

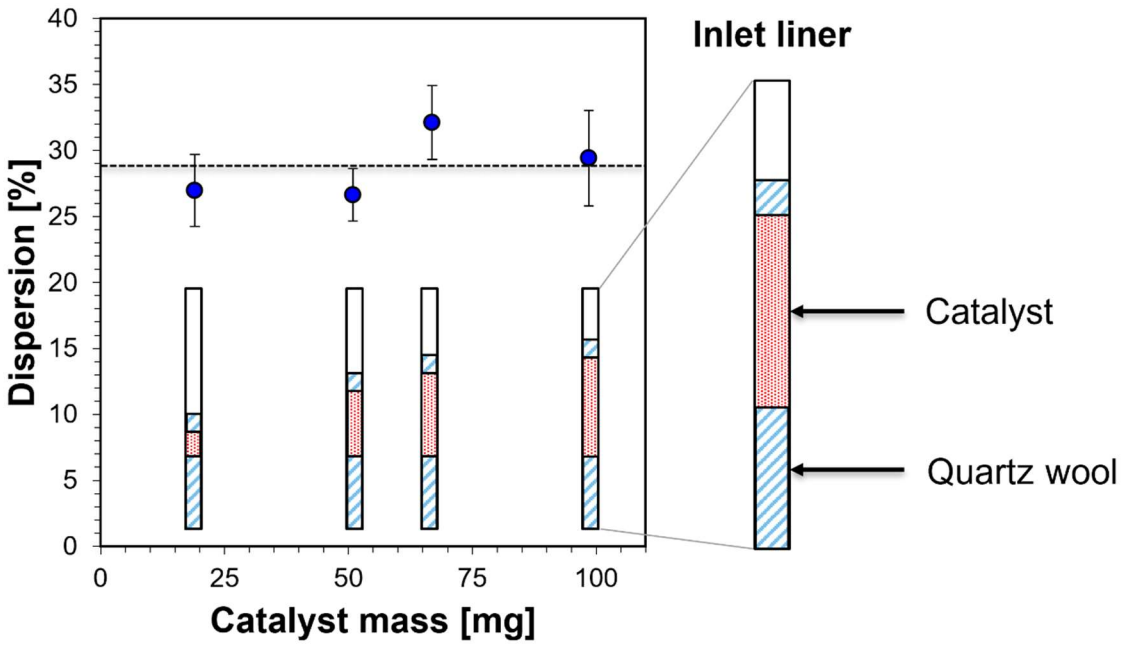

Figure 6: Dispersion of 1 wt % platinum on silica at 35°C.

3.6 Dispersion with varying supports and platinum loadings

To extend the technique of chromatographic dynamic chemisorption and verify its applicability over a wide range of catalysts, we chose platinum supported on three commonly used supports - silica, alumina, and carbon. Besides the commercially available catalysts, dispersion measurements using a supported platinum catalyst synthesized via incipient wetness were also carried out. A range of dispersion values for these catalysts were obtained indicating that the applicability of the technique was not limited to a specific range of dispersion as indicated in Table 1. Reliable dispersion estimations were obtained to quantify the amount of dispersed metal varying across an order of magnitude from 0.02 mg to 0.33 mg. to A variability in dispersion values in all the cases indicates that the dispersion is a strong function of the metal loading as well as the support identity used. Besides, support-metal interaction also governs the extent of dispersion of the catalysts.[65,

[66] The properties of the oxide support such as its isoelectric point also govern the extent of dispersion of the metal particles on its surface.

Table 1: Dispersion measurements of supported platinum catalysts

Catalyst	Dispersion (%)
1 wt% Pt/SiO_2	27 ± 2
1 wt% Pt/Al_2O_3	33 ± 3
5 wt% Pt/C	19 ± 1
0.12 wt% Pt/SiO_2	52 ± 5

3.7 Dispersion measurements using standard catalyst

To further confirm the accuracy of dispersion estimations by chromatographic dynamic chemisorption, 0.5 wt% platinum on alumina catalyst provided by the Micromeritics company as a standard for dispersion measurements was used for estimating the dispersion. This catalyst was reported to have a known dispersion value of (33 ± 5) %. Based on our measurements, the dispersion value was estimated to be (29 ± 4) %. This indicates that our measurements agree with what is expected from the commercial instrument within the confidence interval ranges.

3.8 Dispersion measurements using other platinum group metals

Palladium and ruthenium are industrially important platinum group metals.[67, 68] To widen the applicability of chromatographic dynamic dispersion, it was also tested on supported palladium and ruthenium catalysts.

Preliminary measurements for 2 wt% ruthenium on alumina catalyst showed that it took 100 pulses of CO for the catalyst surface to saturate as illustrated in the breakthrough profile in Figure 7.

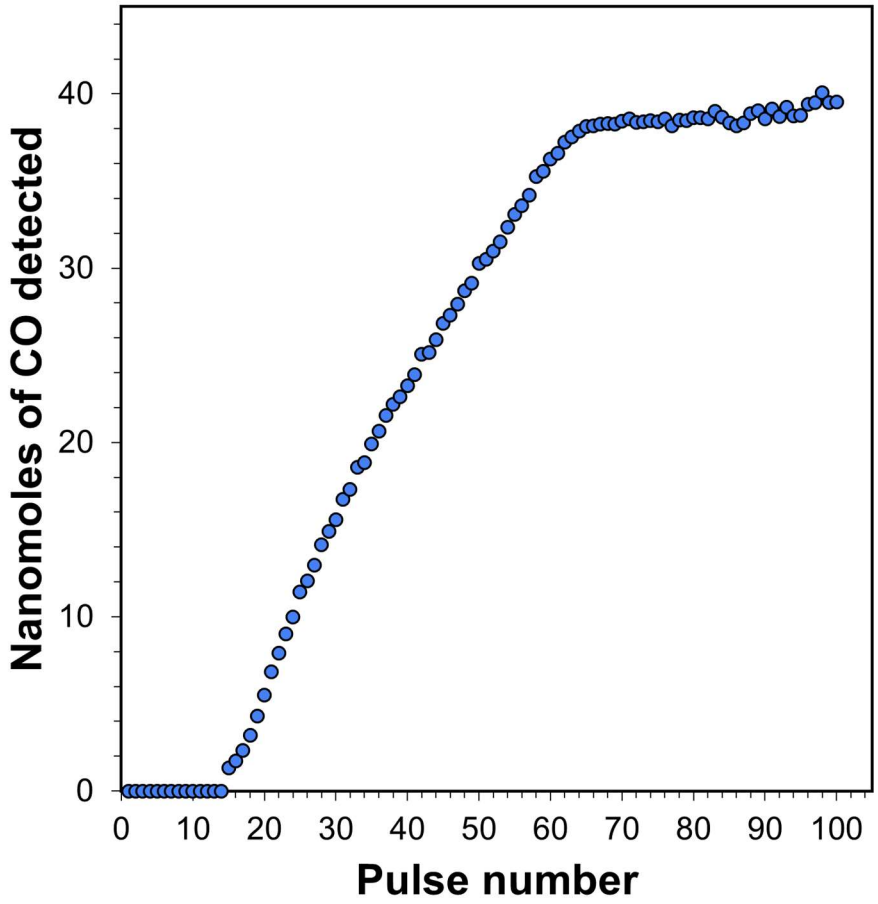

Figure 7: Breakthrough profile of CO adsorption on 2 wt% ruthenium on alumina. The error bars are not indicated since statistically sufficient measurements were not obtained at these conditions for error analysis.

The physical properties of this catalyst such as the porosity might result in diffusion mass transfer limitations resulting in an increased number of pulses required in the region between complete adsorption and saturation of the catalyst. The diffusion limitations might also result in channeling of CO through the catalyst bed. This could explain the shape of

the breakthrough profile in Figure 7 where small amount of CO is adsorbed in each pulse after complete adsorption until the catalyst is saturated as opposed to sharp S-shaped curves observed with platinum catalysts as shown in Figure 3. The dispersion estimated was 62 % translating to 0.63 mg of dispersed metal, the highest relative to all catalysts in this study indicating that this catalyst has the maximum exposed metal surface area. Thus, it is possible that more CO pulses are required to saturate this catalyst compared to all other catalysts since more area is available for adsorption. The amount of catalyst loaded in the bed could be modified to give an amount of dispersed metal in the range at which dispersion measurements have been reliably measured as discussed in Section 3.6. The particle size of the catalyst loaded in the bed can also be modified to check for any significant non-idealities or increased pressure drop across the bed which could distort the breakthrough profile.

5 wt% palladium on carbon catalyst showed similar behavior as 5 wt% platinum on carbon catalyst and the dispersion value was estimated to be (9 ± 1) %. The breakthrough profile showed ideal S-shaped curve without any evidence of non-idealities such as bypassing or channeling as shown in Figure 8.

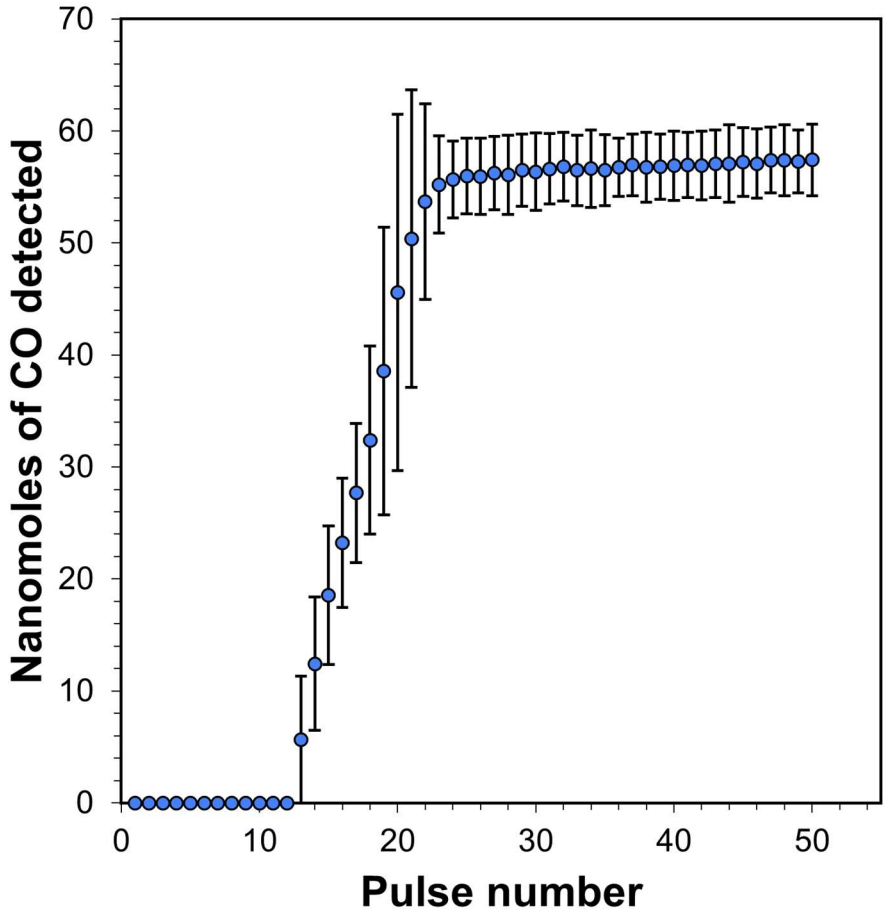

Figure 8: Breakthrough profile for CO pulsed chemisorption on 5 wt% palladium on carbon

CHAPTER 4

SUMMARY AND FUTURE WORK

Dispersion values of supported metal catalysts are required to calculate turn over frequencies or site time yields to allow standardized comparison of catalyst efficacy. The dispersion values of commercially available catalysts are not reported by the manufacturer making it difficult to compare the kinetic data using these catalysts with other catalysts. Hence, dispersion of supported metal catalysts needs to be measured. Several characterization techniques such as transmission electron microscopy, x-ray spectroscopy, and commercially available chemisorption instruments are used to measure dispersion but are limited in their efficiency and accessibility and are expensive.

A simple, cost-effective, and accessible technique to measure catalyst dispersion using a gas chromatograph using the principle of dynamic pulsed chemisorption is proposed. The inlet of the gas chromatograph contains the catalyst as a bed through which known amount of CO pulsed, the column screens for any impurities and the detector quantifies the unadsorbed CO. The catalyst was pre-treated insitu and purged with an inert carrier gas before chemisorption measurements were carried out. The pre-treatment, purge, and CO chemisorption methods were sequenced using the chemstation software available with the gas chromatograph to ensure complete automation of the process. A breakthrough profile of the CO as it saturates the catalyst bed wass obtained. The difference between the pulsed and detected CO gives the amount of adsorbed CO which wass translated to amount of exposed metal surface atoms using the stoichiometry factor. There was no variation in the dispersion measured using this technique with temperature ranging from 35 ^{o}C to 50 ^{o}C indicating no CO adsorbed on the support. No variation in dispersion measurements

with variation in catalyst mass from 19 mg to 99 mg was observed and expected since dispersion is an intensive quantity. Significant variation of dispersion was observed with changes in weight loading or support identity of the supported metal catalyst as suggested by the literature. The accuracy of the technique was tested using a standard catalyst of known dispersion, measured and reported values of dispersion were the same within 95% confidence interval.

The amount of catalyst that can be analyzed for dispersion estimation is limited to the bed volume of 0.35 cm^3 due to the fixed diameter of the inlet liner and to ensure temperature gradient <5 K across the bed length. Reliable measurements for amount of dispersed metal ranging from 0.02 mg to 0.33 mg were obtained but obtaining dispersion estimations outside this range could be challenging due to bed volume limitations. Additionally, chromatographic dynamic chemisorption cannot distinguish between the different types of active sites on the catalyst.

To further extend the applicability of the proposed technique, studies can be conducted to expand the database of dispersion of commercial catalysts. The effects of physical properties of the catalyst on the method parameters and how it influences the accuracy of dispersion estimation can be examined. The test of efficiency of the proposed technique is limited to measuring the dispersion value of a standard catalyst as described in Section 3.7. To increase the confidence in dispersion estimations using this technique and comment on the relative sensitivity of the proposed technique and commercial instruments, more comparisons would be required. Thus, measurement of dispersion values using a commercially available instrument for the same catalyst samples whose

dispersion was estimated by the proposed technique would serve as an additional check to test the efficiency and reliability of the technique.

Chromatographic dynamic chemisorption is developed with the goal of availing an inexpensive and accessible dispersion estimation technique for supported metal catalysts (commercially available and synthesized) for catalysis research. Thus, a gas chromatograph, ubiquitous in catalysis research, is exploited to realize this goal. The technique is tested for its reliability across various parameters and can be potentially used for estimating dispersion of all supported metal catalysts.

REFERENCES

1. Curry, S. W., Platinum catalysts in Petroleum refining. *Platinum metals review* **1957,** *1* (2), 38-43.
2. Ma, Z.; Wei, L.; Zhou, W.; Jia, L.; Hou, B.; Li, D.; Zhao, Y. J. R. a., Overview of catalyst application in petroleum refinery for biomass catalytic pyrolysis and bio-oil upgrading. **2015,** *5* (107), 88287-88297.
3. Hayler, J. D.; Leahy, D. K.; Simmons, E. M., A Pharmaceutical Industry Perspective on Sustainable Metal Catalysis. *Organometallics* **2019,** *38* (1), 36-46.
4. Liu, M.; Wang, L.; Zhao, K.; Shi, S.; Shao, Q.; Zhang, L.; Sun, X.; Zhao, Y.; Zhang, J. J. E.; Science, E., Atomically dispersed metal catalysts for the oxygen reduction reaction: synthesis, characterization, reaction mechanisms and electrochemical energy applications. **2019,** *12* (10), 2890-2923.
5. Ford, D. C.; Nilekar, A. U.; Xu, Y.; Mavrikakis, M. J. S. S., Partial and complete reduction of O2 by hydrogen on transition metal surfaces. **2010,** *604* (19-20), 1565-1575.
6. Ford, D.; Xu, Y.; Mavrikakis, M., Atomic and molecular adsorption on Pt(1 1 1). *Surface Science - SURFACE SCI* **2005,** *587*, 159-174.
7. Hughes, A. E.; Haque, N.; Northey, S. A.; Giddey, S. J. R., Platinum Group Metals: A Review of Resources, Production and Usage with a Focus on Catalysts. **2021,** *10* (9), 93.
8. Ndolomingo, M. J.; Bingwa, N.; Meijboom, R. J. J. o. M. S., Review of supported metal nanoparticles: synthesis methodologies, advantages and application as catalysts. **2020,** *55* (15), 6195-6241.
9. Saqer, S. M.; Kondarides, D. I.; Verykios, X. E. J. T. i. C., Catalytic activity of supported platinum and metal oxide catalysts for toluene oxidation. **2009,** *52* (5), 517-527.
10. Tauster, S.; Fung, S.; Baker, R.; Horsley, J. J. S., Strong interactions in supported-metal catalysts. **1981,** *211* (4487), 1121-1125.
11. Pinna, F. J. C. T., Supported metal catalysts preparation. **1998,** *41* (1-3), 129-137.
12. Chorkendorff, I.; Niemantsverdriet, J. W., *Concepts of modern catalysis and kinetics*. John Wiley & Sons: 2017.
13. Somorjai, G. A.; Carrazza, J. J. I.; fundamentals, e. c., Structure sensitivity of catalytic reactions. **1986,** *25* (1), 63-69.
14. Boudart, M.; Aldag, A.; Benson, J.; Dougharty, N.; Harkins, C. G. J. J. o. c., On the specific activity of platinum catalysts. **1966,** *6* (1), 92-99.
15. Davis, M. E.; Davis, R. J., *Fundamentals of chemical reaction engineering*. Courier Corporation: 2012.
16. Chalk, S. J., The IUPAC Gold Book website. **2019**.
17. Cortright, R. D.; Goddard, S. A.; Rekoske, J. E.; Dumesic, J. J. J. o. c., Kinetic study of ethylene hydrogenation. **1991,** *127* (1), 342-353.
18. Goddard, S. A.; Cortright, R. D.; Dumesic, J. J. J. o. C., Deuterium tracing studies and microkinetic analysis of ethylene hydrogenation over platinum. **1992,** *137* (1), 186-198.
19. Abdelrahman, O. A.; Heyden, A.; Bond, J. Q. J. A. c., Analysis of kinetics and reaction pathways in the aqueous-phase hydrogenation of levulinic acid to form γ-valerolactone over Ru/C. **2014,** *4* (4), 1171-1181.

20. Abdelrahman, O. A.; Luo, H. Y.; Heyden, A.; Román-Leshkov, Y.; Bond, J. Q. J. J. o. c., Toward rational design of stable, supported metal catalysts for aqueous-phase processing: Insights from the hydrogenation of levulinic acid. **2015,** *329*, 10-21.
21. Zhang, W.; Wang, H.; Jiang, J.; Sui, Z.; Zhu, Y.; Chen, D.; Zhou, X., Size Dependence of Pt Catalysts for Propane Dehydrogenation: from Atomically Dispersed to Nanoparticles. *ACS Catalysis* **2020,** *10* (21), 12932-12942.
22. Sanyal, U.; Song, Y.; Singh, N.; Fulton, J. L.; Herranz, J.; Jentys, A.; Gutiérrez, O. Y.; Lercher, J. A., Structure Sensitivity in Hydrogenation Reactions on Pt/C in Aqueous-phase. *ChemCatChem* **2019,** *11* (1), 575-582.
23. Mehrabadi, B. A. T.; Eskandari, S.; Khan, U.; White, R. D.; Regalbuto, J. R., Chapter One - A Review of Preparation Methods for Supported Metal Catalysts. In *Advances in Catalysis*, Song, C., Ed. Academic Press: 2017; Vol. 61, pp 1-35.
24. Corella, J.; Toledo, J. M.; Padilla, A. M., On the selection of the catalyst among the commercial platinum-based ones for total oxidation of some chlorinated hydrocarbons. *Applied Catalysis B: Environmental* **2000,** *27* (4), 243-256.
25. Van Trimpont, P.; Marin, G.; Froment, G. J. I.; research, e. c., Reforming of C7 hydrocarbons on a sulfided commercial platinum/alumina catalyst. **1988,** *27* (1), 51-57.
26. Manta, C. M.; Bozga, G.; Bercaru, G.; Bîldea, C. S., Kinetics of o-Xylene Combustion over a Pt/Alumina Catalyst. *Chemical Engineering & Technology* **2012,** *35* (12), 2147-2154.
27. Leofanti, G.; Tozzola, G.; Padovan, M.; Petrini, G.; Bordiga, S.; Zecchina, A., Catalyst characterization: characterization techniques. *Catalysis Today* **1997,** *34* (3), 307-327.
28. Avci, A. K.; Önsan, Z. I., 2.16 Catalysts. In *Comprehensive Energy Systems*, 2018; pp 475-523.
29. Thomas, J. M., Reflections on the value of electron microscopy in the study of heterogeneous catalysts. *Proceedings of the Royal Society A: Mathematical, Physical and Engineering Sciences* **2017,** *473* (2197), 20160714.
30. Rioux, R.; Song, H.; Grass, M.; Habas, S.; Niesz, K.; Hoefelmeyer, J.; Yang, P.; Somorjai, G. J. T. i. C., Monodisperse platinum nanoparticles of well-defined shape: synthesis, characterization, catalytic properties and future prospects. **2006,** *39* (3), 167-174.
31. Rodríguez-Reinoso, F.; Rodríguez-Ramos, I.; Moreno-Castilla, C.; Guerrero-Ruiz, A.; López-González, J. J. J. o. C., Platinum catalysts supported on activated carbons: I. Preparation and characterization. **1986,** *99* (1), 171-183.
32. Williams, D. B.; Carter, C. B., The Transmission Electron Microscope. In *Transmission Electron Microscopy: A Textbook for Materials Science*, Williams, D. B.; Carter, C. B., Eds. Springer US: Boston, MA, 1996; pp 3-17.
33. Wang, Y.; Niu, Y.; Gao, T.; Liu, S.; Zhang, B., Assessing the Effect of the Electron-Beam Irradiation on Pd/Ga2O3 Catalyst under Ambient Pressure. *ChemCatChem* **2020,** *12* (19), 4765-4769.
34. Chen, M.; Cai, Y.; Yan, Z.; Gath, K.; Axnanda, S.; Goodman, D. W. J. S. S., Highly active surfaces for CO oxidation on Rh, Pd, and Pt. **2007,** *601* (23), 5326-5331.
35. Rupprechter, G. J. A. R. S. C., 8 Surface vibrational spectroscopy on noble metal catalysts from ultrahigh vacuum to atmospheric pressure. **2004,** *100*, 237-311.
36. Taglauer, E., Surface Chemical Composition. *Handbook of Heterogeneous Catalysis* **2008**, 1014-1029.

37. Ratner, B. D.; Castner, D. G., Electron Spectroscopy for Chemical Analysis. *Surface Analysis – The Principal Techniques* **2009**, 47-112.
38. Tarditi, A. M.; Mori, M. F.; Cornaglia, L. M., Determination of the Metal Dispersion of Supported Catalysts Using XPS. *Topics in Catalysis* **2019,** *62* (12), 822-837.
39. Kerkhof, F. P. J.; Moulijn, J. A., QUANTITATIVE ANALYSIS OF XPS INTENSITIES FOR SUPPORTED CATALYSTS. **1979**.
40. Davis, S. M., Particle size information from dispersed phase photoemission intensity ratios. *Journal of Catalysis* **1989,** *117* (2), 432-446.
41. Yano, J.; Yachandra, V. K., X-ray absorption spectroscopy. *Photosynthesis Research* **2009,** *102* (2), 241.
42. de Graaf, J.; van Dillen, A. J.; de Jong, K. P.; Koningsberger, D. C., Preparation of Highly Dispersed Pt Particles in Zeolite Y with a Narrow Particle Size Distribution: Characterization by Hydrogen Chemisorption, TEM, EXAFS Spectroscopy, and Particle Modeling. *Journal of Catalysis* **2001,** *203* (2), 307-321.
43. Le Valant, A.; Comminges, C.; Can, F.; Thomas, K.; Houalla, M.; Epron, F., Platinum Supported Catalysts: Predictive CO and H2 Chemisorption by a Statistical Cuboctahedron Cluster Model. *The Journal of Physical Chemistry C* **2016,** *120* (46), 26374-26385.
44. Webb, P. A. J. M. I. C. T. P., Introduction to chemical adsorption analytical techniques and their applications to catalysis. **2003**.
45. Fadoni, M.; Lucarelli, L. J. S. i. s. s.; catalysis, Temperature programmed desorption, reduction, oxidation and flow chemisorption for the characterisation of heterogeneous catalysts. Theoretical aspects, instrumentation and applications. **1999,** *120*, 177-225.
46. Li, X.; Shen, Y.; Xing, R.; Liu, Y.; Wu, H.; He, M.; Wu, P. J. C. l., Effective and reusable Pt catalysts supported on periodic mesoporous resols for chiral hydrogenation. **2008,** *122* (3), 325-329.
47. Karakaya, C.; Deutschmann, O. J. A. C. A. G., A simple method for CO chemisorption studies under continuous flow: Adsorption and desorption behavior of Pt/Al2O3 catalysts. **2012,** *445*, 221-230.
48. Wang, R., Fabrication and testing of low-temperature catalytically active washcoat materials for next-generation vehicle catalytic converters. **2014**.
49. Domínguez-Domínguez, S.; Berenguer-Murcia, Á.; Linares-Solano, Á.; Cazorla-Amorós, D. J. J. o. C., Inorganic materials as supports for palladium nanoparticles: Application in the semi-hydrogenation of phenylacetylene. **2008,** *257* (1), 87-95.
50. Hussain, M.; Song, S.-K.; Ihm, S.-K., Synthesis of hydrothermally stable MCM-41 by the seed crystallization and its application as a catalyst support for hydrodesulfurization. *Fuel* **2013,** *106*, 787-792.
51. Souza, M. M. V. M.; Schmal, M., Methane Conversion to Synthesis Gas by Partial Oxidation and CO2 Reforming over Supported Platinum Catalysts. *Catalysis Letters* **2003,** *91* (1), 11-17.
52. Pramhaas, V.; Roiaz, M.; Bosio, N.; Corva, M.; Rameshan, C.; Vesselli, E.; Grönbeck, H.; Rupprechter, G., Interplay between CO Disproportionation and Oxidation: On the Origin of the CO Reaction Onset on Atomic Layer Deposition-Grown Pt/ZrO2 Model Catalysts. *ACS Catalysis* **2021,** *11* (1), 208-214.

53. Foger, K.; Anderson, J. R., Temperature programmed desorption of carbon monoxide adsorbed on supported platinum catalysts. *Applications of Surface Science* **1979,** *2* (3), 335-351.
54. Sietsma, J. R. A.; Jos van Dillen, A.; de Jongh, P. E.; de Jong, K. P., Application of ordered mesoporous materials as model supports to study catalyst preparation by impregnation and drying. In *Studies in Surface Science and Catalysis*, Gaigneaux, E. M.; Devillers, M.; De Vos, D. E.; Hermans, S.; Jacobs, P. A.; Martens, J. A.; Ruiz, P., Eds. Elsevier: 2006; Vol. 162, pp 95-102.
55. Mcminn, D. In *CHROMATOGRAPHY: GAS | Detectors: General (Flame Ionization Detectors and Thermal Conductivity Detectors)*, 2000.
56. Grossman, S., It's a Matter of Degrees, but Do Degrees Really Matter?. An Observation of GC Inlet Temperature Profile and Inlet-to-Inlet Temperature Variability **2013**.
57. Poole, C. F., GAS CHROMATOGRAPHY | Detectors. In *Encyclopedia of Analytical Science (Second Edition)*, Worsfold, P.; Townshend, A.; Poole, C., Eds. Elsevier: Oxford, 2005; pp 95-105.
58. Chapter 16 Quantitative Analysis By Gas Chromatography Sources of Errors, Accuracy and Precision of Chromatographic Measurements. In *Journal of Chromatography Library*, Guiochon, G.; Guillemin, C. L., Eds. Elsevier: 1988; Vol. 42, pp 661-687.
59. Asadi, M.; Xie, G.; Sunden, B., A review of heat transfer and pressure drop characteristics of single and two-phase microchannels. *International Journal of Heat and Mass Transfer* **2014,** *79*, 34-53.
60. Thrush, K. A.; White, J. M., Carbon monoxide and hydrogen coadsorption on polycrystalline platinum. *Applied Surface Science* **1985,** *24* (1), 108-120.
61. Nishiyama, Y.; Wise, H., Surface interactions between chemisorbed species on platinum: Carbon monoxide, hydrogen, oxygen, and methanol. *Journal of Catalysis* **1974,** *32* (1), 50-62.
62. Bashlakov, D. L.; Juurlink, L. B. F.; Koper, M. T. M.; Yanson, A. I., Subsurface Oxygen on Pt(111) and Its Reactivity for CO Oxidation. *Catalysis Letters* **2012,** *142* (1), 1-6.
63. Levenspiel, O., *Chemical reaction engineering*. John wiley & sons: 1998.
64. Gabelman, A. J. C. E. P., Adsorption basics: part 1. **2017,** *113* (7), 48-53.
65. Parapat, R. Y.; Saputra, O. H. I.; Ang, A. P.; Schwarze, M.; Schomäcker, R., Support effect in the preparation of supported metal catalysts via microemulsion. *RSC Advances* **2014,** *4* (92), 50955-50963.
66. Lokteva, E. S.; Golubina, E. V., Metal-support interactions in the design of heterogeneous catalysts for redox processes %J Pure and Applied Chemistry. **2019,** *91* (4), 609-631.
67. Wang, S.; Schrunk, E. T.; Mahajan, H.; Farrauto; J., R., The Role of Ruthenium in CO2 Capture and Catalytic Conversion to Fuel by Dual Function Materials (DFM). **2017,** *7* (3), 88.
68. Zhang, L.; Song, Q.; Liu, Y.; Xu, Z., Novel approach for recovery of palladium in spent catalyst from automobile by a capture technology of eutectic copper. *Journal of Cleaner Production* **2019,** *239*, 118093.